

# Diversity in Biology: definitions, quantification and models

Song Xu<sup>1</sup>, Lucas Böttcher<sup>2</sup>, and Tom Chou<sup>3</sup>

<sup>1</sup>Center for Biomedical Informatics Research, Department of Medicine, Stanford University, Stanford, California

<sup>2</sup>Institute for Theoretical Physics and Center of Economic Research, ETH Zurich, Zurich, Switzerland

<sup>3</sup>Department of Mathematics, UCLA, Los Angeles, CA 90095-1766

E-mail: tomchou@ucla.edu

**Abstract.** Diversity indices are useful single-number metrics for characterizing a complex distribution of a set of attributes across a population of interest. The utility of these different metrics or set of metrics depend on the context and application, and whether a predictive mechanistic model exists. In this topical review, we outline the various definitions of “diversity” and provide examples of scientific topics in which its quantification plays an important role. We review how diversity is a ubiquitous concept across multiple fields including ecology, immunology, cellular barcoding studies, and social economic studies. Since many of these applications involve sampling of populations, we also review how diversity in small samples is related to the diversity in the entire population. Features that arise in each of these applications are highlighted.

*Keywords:* diversity indices, information theory, Shannon index, sampling, barcoding, ecology, microbiota, immunology, wealth distributions

Submitted to: *Physical Biology*

## 1. Introduction

“Diversity” is a frequently used concept across a broad spectrum of scientific disciplines, ranging from biology [1, 2, 3, 4, 5] and ecology [6, 7, 8, 9, 10, 11], over investment and portfolio theory [12, 13, 14, 15, 16], to linguistics [17, 18] and sociology [19, 20, 21, 22, 23, 24]. In each of these disciplines, diversity is a measure of the range and distribution of certain features within a given population. It is considered a key attribute that can be dynamically varying, influenced by intra-population interactions, and modified by environmental factors. The concept of diversity, variety, or heterogeneity can be applied to any population. The evolution of the population can also be highly correlated with its diversity. Some examples of biological population dynamics occurring at different scales are shown in Fig. 1. At first sight, diversity seems to be an intuitively simple concept, but since certain population attributes require a full distribution function to quantify, it can be rather complex and difficult to capture using a single metric [25, 3, 4, 26]. We could for example think of a community with a total of four species, with one of the species dominating the total population. Consider a second community that consists of two equally common species. Which one of the two communities exhibits a higher diversity? The first one, because it harbors a larger number of species? Or the second one, because it is more likely a sample is more likely to contain two species? This example shows that diversity is intrinsically linked to the total number of extant species (richness) and how the population is distributed throughout the species (evenness), and thus cannot be captured by a single number [3]. As a result, there are numerous different diversity indices and associated concepts used in different applications [27, 28, 25, 3, 4, 26, 29]. Nonetheless, diversity measures are important for assessing the current condition of ecosystems, to quantify the influence of environmental factors on different species, and in the context of conservation planning [2, 9, 30, 5, 31, 10, 29]. In addition, the concept of diversity is important for the quantitative description of wealth distributions and, more generally, to identify mechanisms leading to variations in societies [32, 33, 34, 35, 36]. In a broader sense, diversity indices may be helpful for the design of robust energy distribution systems [37] or even to assemble well-performing teams [23]. Thus we see that, despite the ambiguity in the definition of diversity, the concept is very relevant to many different disciplines and applications.

In this topical review, we start by summarizing the basic concepts from information theory which are necessary for a quantitative treatment of diversity. We continue with describing aspects of populations

and diversity that are common to many applications in biology. In the next section, we present the common mathematical descriptions of diversity in terms of both number and species counts. Moreover, most applications, only a small sample of a population is available. Thus, we place particular emphasis on the effects of sampling on diversity measures in Section 4. In the following section and subsections, we survey a number of biological systems in which concepts of diversity play a key role in understanding the dynamics of the population. These include ecological populations, stem cell barcoding experiments, immunology, cancer, and societal wealth distributions. Each of these systems carry their unique attributes and thus require specific diversity measures. Finally, in Section 6 we conclude with a discussion of possible future applications of concepts of diversity.

## 2. Mathematical Concepts

### 2.1. Entropy, relative entropy, KL divergence, KS statistic, mutual information and all that

Common notions that arise in the analysis of diversity naturally seek to quantitatively compare distributions and invariably involve ideas from information theory. In this context, we may think of terms such as entropy and mutual information which carry a rich history with deep connections to thermodynamics, coding theory, cryptography, inference, and communication [38]. To review the necessary information-theoretic concepts, we consider a discrete random variable  $X$  which takes on values from the set  $\{x_1, x_2, \dots, x_N\}$  with probability  $P(x_k) = \Pr(X = x_k)$  such that

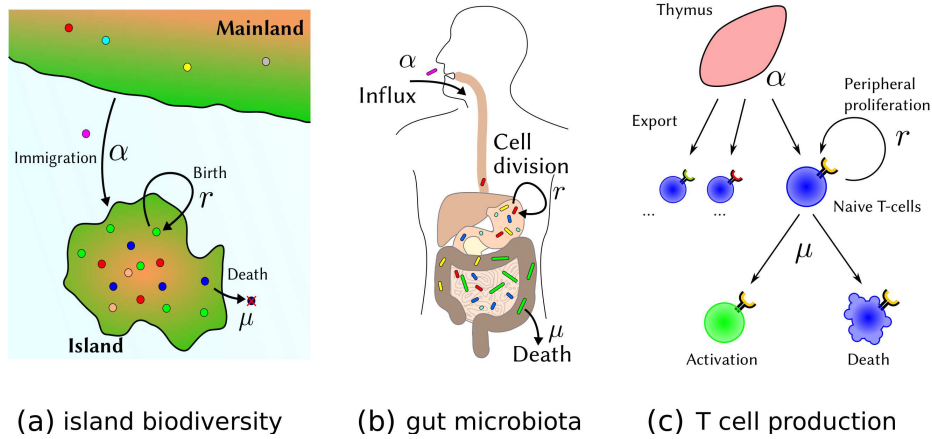
$$\sum_{k=1}^N P(x_k) = 1, \quad (1)$$

where the sum is taken over all possible values  $x_k$ . In the case of species diversity, we may interpret the probability mass function  $P(x_k)$  as the proportion of species  $x_k$  in a certain community. The entropy, or *Shannon entropy* is defined by

$$H(X) = - \sum_{k=1}^N P(x_k) \log P(x_k). \quad (2)$$

and can be thought of as the expected uncertainty or surprise  $-\mathbb{E}[\log P(X)]$ .

The continuous limit of Shannon entropy, or *differential Shannon entropy* has also been defined, but care must be taken if  $X$  carries physical dimensions. If the probability of  $X$  taking on values in the interval  $[x, x + dx]$  is denoted by  $P(x)dx$ , the simplistic extension of Shannon entropy to  $H(X) \sim - \int P(x) \log P(x) dx$  involves a logarithm of a quantity with dimensions  $X^{-1}$ . However, one can take a



(a) island biodiversity (b) gut microbiota (c) T cell production

**Figure 1.** (a) Diversity in island ecology. A large number of species may migrate onto an island. Organisms can proliferate and die, leading to a specific time-dependent pattern of species diversity on the island. (b) Microbes are ingested and form a community in the gut by proliferating, competing, and dying. They can also be cleared from the gut. (c) Naive T cell generation in vertebrates. Naive T cells develop in the thymus. Each T cell expresses only one type of T cell receptor (TCR). Naive T cells can proliferate and die in the peripheral blood. The possible number of T cell receptors that can be expressed is enormous  $> 10^{15}$ , but only perhaps  $10^6 - 10^8$  different TCRs typically exist in an organism. The diversity of the T cell receptor repertoire is an important determinant of the organism's response to antigens.

limiting density of discrete points and define an invariant measure by

$$\lim_{N \rightarrow \infty} \frac{\#\text{points} \in [a, b]}{N} \equiv \int_a^b P_0(x) dx, \quad (3)$$

where  $P_0(x)$  denotes the corresponding point density function. Thus, a limiting Shannon entropy can be defined as [39]

$$\lim_{N \rightarrow \infty} H_N(X) \sim - \int P(x) \log \left( \frac{P(x)}{P_0(x)} \right) dx. \quad (4)$$

These expressions are synonymous with the *Shannon index* of species diversity with some freedom in the choice of the base of the logarithm. Since  $H(X)$  is typically smaller for peaked distributions, and larger for flatter distributions, the Shannon index can serve as a measure of diversity [40].

To characterize the diversity between two communities, we consider two discrete random variables  $X$  and  $Y$  with the corresponding joint probability mass function  $P_{X,Y}(x_k, y_\ell) = \Pr(X = x_k, Y = y_\ell)$ . Given the joint distribution  $P_{X,Y}(x_k, y_\ell)$ , we are able to compute the marginal distributions  $P_X(x_k) = \sum_\ell P_{X,Y}(x_k, y_\ell)$  and  $P_Y(y_\ell) = \sum_k P_{X,Y}(x_k, y_\ell)$  by summing over marginalizing out the complementary variable. These definitions enable us to define the joint entropy

$$H(X, Y) = - \sum_{k, \ell} P_{X,Y}(x_k, y_\ell) \log P_{X,Y}(x_k, y_\ell), \quad (5)$$

which may be also written as  $-\mathbb{E}[\log P_{X,Y}]$ . Moreover, the conditional entropy

$$H(Y|X) = - \sum_{k, \ell} P_{X,Y}(x_k, y_\ell) \log \left( \frac{P_{X,Y}(x_k, y_\ell)}{P_X(x_k)} \right) \quad (6)$$

$$= - \sum_{k, \ell} P_{X,Y}(x_k, y_\ell) \log P_{X|Y}(x_k|y_\ell) \quad (7)$$

describes the expected uncertainty in the random variable  $Y$  given  $X$ . It can be also expressed as  $-\mathbb{E}[\log P_{X|Y}]$  where  $P_{X|Y}$  is the conditional probability mass function. For independent random variables  $X$  and  $Y$ , we find that  $H(Y|X) = H(Y)$  and  $H(X|Y) = H(X)$ .

While the Shannon index is a measure of the absolute entropy of a distribution, the relative entropy or Kullback-Leibler (KL) divergence

$$\begin{aligned} D_{\text{KL}}(P||Q) &= \sum_k P(x_k) \log \left( \frac{P(x_k)}{Q(x_k)} \right) \\ &= \mathbb{E}_P [\log P(x_k) - \log Q(x_k)], \end{aligned} \quad (8)$$

quantifies the distance between two probability mass functions  $P$  and  $Q$ . In the case of continuous distributions  $P(x)$  and  $Q(x)$ , we obtain  $D_{\text{KL}}(P||Q) = \int P(x) \log(P(x)/Q(x)) dx$ .

The KL divergence is the relative entropy of  $P$  with respect to the reference distribution  $Q$ . Note that the limiting Shannon entropy is simply the KL divergence between the distribution  $P(x)$  and the associated invariant measure  $P_0(x)$ . Typically,  $P$  is an experimental or observed distribution and  $Q$  is a model that represents  $P$ . Furthermore, the KL divergence is nonnegative and equals zero if and only if  $P = Q$  [38]. It is not symmetric,  $D_{\text{KL}}(P||Q) \neq D_{\text{KL}}(Q||P)$ , and is thus not a metric. In addition, a special case of the KL divergence is *mutual information*

$$\begin{aligned} I(X; Y) &= D_{\text{KL}}(P_{X,Y} || P_X P_Y), \\ &= \sum_{k, \ell} P_{X,Y}(x_k, y_\ell) \log \left( \frac{P_{X,Y}(x_k, y_\ell)}{P_X(x_k) P_Y(y_\ell)} \right). \end{aligned} \quad (9)$$

Note that  $I(X;Y) = I(Y;X)$  is symmetric and quantifies how much knowing one variable reduces the uncertainty in the other. If  $X$  and  $Y$  are completely independent,  $I(X,Y) = 0$ . According to Eq. (9) and the definitions of joint and conditional entropy in Eqs. (7) and (5), the mutual information can be written in terms of marginal, conditional, and joint entropies [38]:

$$\begin{aligned} I(X;Y) &= H(X) - H(X|Y) = H(Y) - H(Y|X) \\ &= H(X) + H(Y) - H(X,Y). \end{aligned} \quad (10)$$

A symmetric version of the KL divergence is provided by the Jensen-Shannon divergence [41]

$$\text{JSD}(P\|Q) = \frac{1}{2}D_{\text{KL}}(P\|M) + \frac{1}{2}D_{\text{KL}}(Q\|M), \quad (11)$$

where  $M = (P + Q)/2$  defines the mean distribution of  $P$  and  $Q$ . These divergences can be extended to include multiple and higher dimensional distributions. The square-root of the Jensen-Shannon divergence is a distance metric between two distributions.

Another useful distance metric is the Kolmogorov-Smirnov (KS) distance, which is defined as

$$D_{\text{KS}} = \max_x |G(x) - F(x)|, \quad (12)$$

where  $F(x)$  and  $G(x)$  denote the cumulative reference and cumulative sample or test distribution, respectively. The distribution  $G(x)$  is based on different realizations drawn from the same underlying distribution  $F(x)$  or from another distribution to be tested against  $G(x)$ . The KS metric is the maximum distance between two cumulative distributions. We outline in Sec. 5.6 that the KS metric is related to the Hoover index which is used to quantify diversity, or inequity, in wealth or income distributions relative to a uniform distribution.

### 3. Measures of diversity

The notions of entropy and information are naturally related to the spread of a distribution  $P(x)$ , and can be subsumed into a general metric for quantifying diversity. Typically, a population is measured and can be thought of as one realization of an underlying distribution. Consider a realization  $\mathbf{n} = \{n_1, n_2, \dots, n_R\}$  describing the number  $n_i$  of entities of a discrete and distinguishable group/species/type ( $1 \leq i \leq R$ ). The total population is  $N = \sum_{i=1}^R n_i$ . This given realization constitutes a “distribution” across all possible types. Thus, any realization is completely described by a set of  $R$  numbers. One may interpret  $n_i/N$  as the probability or relative frequency  $f_i$  of observing attribute  $i$ .

Diversity measures are a simpler representation of the distribution. An example would be a single parameter which captures the “spread” of the

distribution of realizations  $\{n_i\}$ . This is not different than, for example, defining a Gaussian distribution by its mean and standard deviation. Realizations  $\{n_i\}$ , however, typically are not well-defined functions such as Gaussians. A generalized diversity index has been described in terms of “Hill numbers” of order  $q$  [42, 43, 44]:

$${}^qD = \left( \sum_{i=1}^R f_i^q \right)^{1/(1-q)}, \quad (13)$$

where  $f_i = n_i/N$  is the relative abundance of species  $i$ . This general formula represents different classes of “diversity indices” for different values of  $q$ . It is also useful because one can consistently define an *effective* proportional abundance

$$f_{\text{eff}} := 1/{}^qD = \left( \sum_{i=1}^R f_i^q \right)^{1/(q-1)} \quad (14)$$

that corresponds to an average abundance with increasing weighting towards the larger-population species as  $q$  increases [45, 44].

Note the similarity of this definition to the standard mathematical  $p$ -norm

$$\|\mathbf{f}\|_p := \left( \sum_{i=1}^R f_i^p \right)^{1/p}, \quad (15)$$

except that the exponent is  $1/p$  instead of  $1/(1-q)$ . Another diversity measure is provided by the Renyi index [46]

$${}^qH = \log {}^qD = \frac{1}{1-q} \log \left( \sum_{i=1}^R f_i^q \right), \quad (16)$$

which is a generalization of the Shannon entropy defined in Eq. (2). The order  $q$  describes the sensitivity of  ${}^qD$  and  ${}^qH$  to common and rare species [47]. Below, we provide an overview of the most commonly used indices which result from the generalized diversity  ${}^qD$  for different values of  $q$ :

*Richness.*—In the limit of  $q \rightarrow 0^+$ , the probabilities  $f_i^q$  are equal to unity and  ${}^0D$  is simply the total number of types in the population, or the “richness”  $R$ . The richness is often used in quantifying the diversity of T cells and species counts in ecology [3].

*Shannon index.*—For  $q = 1 - \varepsilon$  in the limit  $\varepsilon \rightarrow 0^+$ , the generalized diversity as defined by Eq. (15) becomes

$$\begin{aligned} {}^1D &= \lim_{\varepsilon \rightarrow 0^+} \left( \sum_{i=1}^R f_i^{1-\varepsilon} \right)^{-1/\varepsilon} = \lim_{\varepsilon \rightarrow 0^+} \left( \sum_{i=1}^R f_i e^{-\varepsilon \ln f_i} \right)^{-1/\varepsilon} \\ &= \lim_{\varepsilon \rightarrow 0^+} \left( \sum_{i=1}^R f_i (1 - \varepsilon \ln f_i + O(\varepsilon^2)) \right)^{-1/\varepsilon} \end{aligned}$$

$$\begin{aligned}
 &= \lim_{\varepsilon \rightarrow 0^+} \left( 1 - \varepsilon \sum_{i=1}^R f_i \ln f_i \right)^{-1/\varepsilon} \\
 &= \exp \left[ - \sum_{i=1}^R f_i \ln f_i \right], \tag{17}
 \end{aligned}$$

which is the exponentiation of the Shannon index

$$\text{Sh} := \ln \left( \lim_{q \rightarrow 1^-} {}^q D \right) = - \sum_{i=1}^R f_i \log f_i \tag{18}$$

that parallels the Shannon entropy defined in Eqs. (2) and (7). This index is also sometimes called the Shannon-Wiener index ( $H$ ) and can be defined using any logarithmic base. Typically measured values are  $\text{Sh} \sim \mathcal{O}(1)$ . Qualitatively,  $e^{\text{Sh}}$  can be thought of as a rule of thumb for the number of effective species in a population.

*Evenness.*—Evenness is another class of diversity indices often invoked in ecological and sociological studies. One definition (“Shannon’s equability”) is based on simply normalizing the Shannon diversity by the maximum Shannon diversity that arises if every species is equally likely [48]:

$$J_E := \frac{\text{Sh}}{\text{Sh}_{\max}} = \frac{\text{Sh}}{\ln R}. \tag{19}$$

*Simpson’s index with replacement.*—When  $q = 2$ , we find

$${}^2 D = 1 / \left( \sum_{i=1}^R f_i^2 \right). \tag{20}$$

Simpson’s diversity index is typically defined as

$$S_r = 1 / {}^2 D = \sum_{i=1}^R f_i^2 = \sum_{i=1}^R \left( \frac{n_i}{N} \right)^2, \tag{21}$$

which carries the interpretation that upon drawing an individual from the population the same species is selected twice.

*Simpson’s index without replacement.*—A related index that cannot be directly constructed from  ${}^q D$  is Simpson’s index *without* replacement:

$$S = \sum_{i=1}^R \frac{n_i(n_i - 1)}{N(N - 1)}. \tag{22}$$

Here, when an individual is drawn, it is not replaced before the second individual is drawn. The differences between  $S_r$  and  $S$  are significant only for systems with small numbers of individuals  $n_i$  for all species  $i$ .

*Berger-Parker diversity index.*—In the  $q \rightarrow \infty$  limit, we find

$${}^\infty D = \lim_{q \rightarrow \infty} \left( \sum_{i=1}^R f_i^q \right)^{1/(1-q)}$$

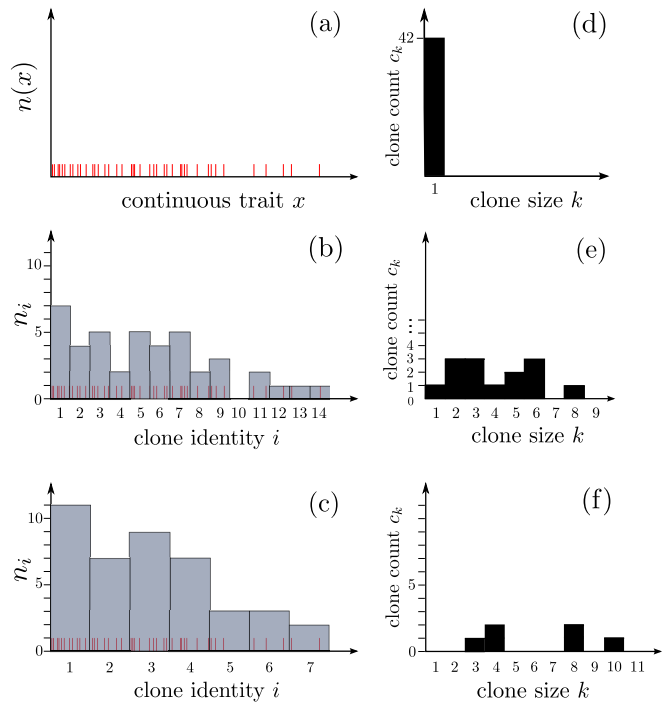


**Figure 2.** Number counts and clone counts vary depending on the definition and thresholding of discrete species. This consideration arises in designing experimental measurements.

$$\begin{aligned}
 &= \lim_{q \rightarrow \infty} f_{\max}^{-\frac{1}{1-1/q}} \left[ \sum_{i=1}^R \left( \frac{f_i}{f_{\max}} \right)^q \right]^{1/(1-q)} \\
 &= f_{\max}^{-1} \tag{23}
 \end{aligned}$$

where  $f_{\max} = \max_{i \in \{1, \dots, R\}}(f_i)$ . The Berger-Parker diversity index

$$1 / {}^\infty D := f_{\max} \tag{24}$$

is defined as the maximum abundance in the set  $\{f_i\}$ , equivalent to the optimal solution of an  $\infty$ -norm of  $\mathbf{f} = \mathbf{n}/N$ .

An alternative way of quantifying a population is through the species abundance distribution or “clone counts” defined by

$$c_k := \sum_{i=1}^R \mathbf{1}(n_i, k) \in \mathbb{Z}^+, \tag{25}$$

where the discrete indicator function  $\mathbf{1}(x, y) = 1$  if  $x = y$  and zero otherwise. The sum is typically taken over all species for which  $n_i \geq 1$ . Clone counts can also be defined over only a certain special subset of species. Clone counts, or species abundance distributions, are thus the discrete level sets of the number counts  $n_i$  that also satisfy

$$N = \sum_{k=1}^{\infty} k c_k \quad \text{and} \quad R = \sum_{k=1}^{\infty} c_k, \tag{26}$$

where  $N$  and  $R$  are the discrete total population and the total number of species (richness) present.

Clone counts are commonly used in the theory of nucleation and self-assembly [49, 50, 51], where all particles are identical and  $c_k$  represents the number of clusters of size  $k$ . They are equivalent to “species abundance distributions” or sometimes ambiguously described as “clone size distributions.” Clone counts have been recently used to quantify populations in barcoding studies [52] described below.

Clone counts do not depend on the specific labeling of the different types  $i$  and do not resolve any identity information. However, since the common diversity indices are only a summary of the vector  $\{n_i\}$  and also do not retain species identity information,  ${}^qD$  can be written in terms of  $c_k$  rather than  $n_i$ :

$${}^qD = \left[ \sum_{k=1}^{\infty} c_k \left( \frac{k}{N} \right)^q \right]^{1/(1-q)}, \quad (27)$$

which leads to corresponding expressions at specific values of  $q$ , e.g.,  ${}^0D = R$ ,

$${}^1D = \exp \left[ - \sum_{k=1}^{\infty} c_k \left( \frac{k}{N} \right) \ln \left( \frac{k}{N} \right) \right] \quad \text{and}$$

$${}^{1/2}D = \sum_{k=1}^{\infty} c_k \left( \frac{k}{N} \right)^2. \quad (28)$$

While the definitions of  ${}^qD$  are well-defined when the discrete species are delineated, for more granular or continuous traits, the delineation of different species will affect the values of  $n_i$  and  $c_k$ . Fig. 2 shows population counts ordered by a continuous trait  $x$ . By defining the discrete species  $i$  according to different binning windows over  $x$ , we find different sets of number and clone counts. Thus, measures of diversity can be highly dependent on the resolution and definition of traits and species.

#### 4. Sampling

In most applications, including all the ones we will discuss below, identification of the entire population is typically not accessible. In an ecology, all animals of the population cannot be tracked. In blood samples, only a small fraction of the cell types in the whole organism is drawn for identification/sequencing. Thus, inferring the diversity in the entire system from the diversity in the sample is a key problem encountered across many fields.

There are numerous ways to randomly sample. One approach is to draw one individual, record its attributes, return it back into the system, and allow it to “equilibrate” before again randomly drawing the next individual. This process can be repeated  $M$  times. To indicate this type of sampling, we use the subscript  $1 \times M$  in the corresponding distributions and expectation values. Similar sampling approaches are

used in the “mark-release-recapture” experiments to estimate population size [53], survival, and dispersal of mosquitos [54]. For a given configuration  $\{n_i\}$  and total population size  $N$  [55], the probability that the configuration  $\{m_i\}$  is drawn after  $M$  samples is simply

$$P_{1 \times M}(\mathbf{m} | \mathbf{n}, M, N) = \binom{M}{m_1, m_2, \dots, m_R} \prod_{j=1}^R f_j^{m_j}, \quad (29)$$

where  $f_j \equiv n_j/N$  is the relative population of species  $i$ ,  $N \equiv \sum_{i=1}^R n_i$  is the total population and  $M \equiv \sum_{i=1}^R m_i$  is the total number of samples.

Using  $P_{1 \times M}$  to find moments of  $m_i$  in terms of Eq. (25), we compute the statistics of how the system diversity is reflected in the diversity in the samples. The lowest moments of the sample configurations are

$$\mathbb{E}_{1 \times M}[m_i] = M f_i = n_i \frac{M}{N}, \quad (30)$$

$$\mathbb{E}_{1 \times M}[m_i m_j] = f_i f_j M(M-1) + f_i M \mathbb{1}(i, j).$$

An alternative random sampling protocol is to draw a fraction  $\sigma \equiv M/N < 1$  of the entire population at once. This type of sampling arises in biopsies, especially in blood lab tests. To be able to distinguish between this sampling protocol and the previous one, we now use the notation  $M \times 1$ . In this case the probability of a specific sample configuration, given  $\mathbf{n}$ ,  $N$ , and  $M$  is, combinatorially,

$$P_{M \times 1}(\mathbf{m} | \mathbf{n}, M, N) = \frac{1}{\binom{N}{M}} \prod_{j=1}^R \binom{n_j}{m_j} \mathbb{1} \left( M, \sum_{i=1}^R m_i \right), \quad (31)$$

where the discrete indicator function enforces the constraint between  $m_i$  and the sampled population  $M$ . In this single-draw sampling scenario, we use  $\mathbb{1}(x, y) \equiv \int_0^{2\pi} \frac{dq}{2\pi} e^{iq(x-y)}$  to find

$$\mathbb{E}_{M \times 1}[m_i] = n_i \frac{M}{N} = n_i \sigma, \quad (32)$$

$$\mathbb{E}_{M \times 1}[m_i m_j] = n_i n_j \frac{M}{N} \frac{M-1}{N-1} + \mathbb{1}(i, j) n_i \frac{M}{N} \left( \frac{N-M}{N-1} \right). \quad (33)$$

Effects of sampling on clone counts  $c_k$  can be similarly calculated. Results using  $P_{1 \times M}$  and  $P_{M \times 1}$  rely on perfectly random sampling, where certain clones/species are not more likely sampled or “captured” than others. The moments  $\mathbb{E}[m_i m_j]$  can be directly used to evaluate the expected Simpson’s diversities,  $S_r$  and  $S$  defined by Eqs. (21) and (22), in the corresponding sample. In the case of  $1 \times M$  sampling, we find

$$\mathbb{E}_{1 \times M}[S_r] = \mathbb{E}_{1 \times M} \left[ \sum_i \left( \frac{m_i}{M} \right)^2 \right]$$

$$\begin{aligned}
&= \frac{M(M-1)}{M^2} \sum_i f_i^2 + \frac{1}{M} \sum_i f_i \\
&= S_r \left(1 - \frac{1}{M}\right) + \frac{1}{M},
\end{aligned} \tag{34}$$

and

$$\begin{aligned}
\mathbb{E}_{1 \times M}[S] &= \mathbb{E}_{1 \times M} \left[ \sum_i \frac{m_i m_i - 1}{M(M-1)} \right] \\
&= \sum_i \frac{\mathbb{E}_{1 \times M}[m_i^2]}{M(M-1)} - \sum_i \frac{\mathbb{E}_{1 \times M}[m_i]}{M(M-1)} \\
&= \sum_i f_i^2 \equiv S
\end{aligned} \tag{35}$$

while for  $M \times 1$  sampling, we find

$$\begin{aligned}
\mathbb{E}_{M \times 1}[S_r] &= \mathbb{E}_{M \times 1} \left[ \sum_i \left( \frac{m_i}{M} \right)^2 \right] \\
&= S_r \frac{M-1}{M-\sigma} + \frac{1-\sigma}{M-\sigma}
\end{aligned} \tag{36}$$

and

$$\begin{aligned}
\mathbb{E}_{M \times 1}[S] &= \mathbb{E}_{M \times 1} \left[ \sum_i \frac{m_i m_i - 1}{M(M-1)} \right] \\
&= \left[ \sum_i \frac{\mathbb{E}_{M \times 1}[m_i^2]}{M(M-1)} - \sum_i \frac{\mathbb{E}_{M \times 1}[m_i]}{M(M-1)} \right] \\
&= S.
\end{aligned} \tag{37}$$

Note that for both types of random sampling, we find that the expected Simpson's diversity (without replacement) in the samples are equal to the Simpson's diversity in the full system.

The above results provide expected diversities in the sample assuming full knowledge of  $\{n_i\}$  in the system. They represent solutions to the "forward" problem, the so-called mean "rarefaction" in ecology. However, the problem of interest is usually the inverse problem, or "extrapolation" in ecology. In the simplest case, we wish to infer the expected diversity (or  $\{n_i\}$  and  $c_k$ ) in the system from a given configuration  $\{m_i\}$  or clone count

$$d_k := \sum_{i=1} \mathbf{1}(m_i, k) \in \mathbb{Z}^+, \tag{38}$$

in the sample(s). Extrapolation is a much harder problem and is the subject of many research papers [56, 57, 58, 59, 60].

One may wish to use the observed sample diversity  ${}^qD(M)$  to approximate the population diversity  ${}^qD(N)$ . For any  $q$ , the underestimation of  ${}^qD(N)$  using  ${}^qD(M)$  decreases as the sample size  $M$  increases. The deviation of  ${}^qD(M)$  from  ${}^qD(N)$  is smaller for larger

$q$ , as higher-order Hill numbers are more heavily weighted by large species, which are less sensitive to subsampling.

Chao and others have shown that for  $q \geq 1$  and in the  $N \rightarrow \infty$  limit nearly unbiased approximations can be obtained and when  $q \geq 2$ , these unbiased estimates are very insensitive to sample size  $M$  [61, 62]. Using clone counts in a sample of population  $M$ , Chao *et al.* [63] obtained for  $q = 1$  (in terms of Shannon's index):

$$\begin{aligned}
\hat{S}h &= \sum_{k=1}^{M-1} \frac{1}{k} \sum_{1 \leq m_i \leq M-k} \frac{m_i}{M} \frac{\binom{M-m_i}{k}}{\binom{M-1}{k}} \\
&+ \frac{d_1}{M} (1-A)^{-M+1} \left\{ -\log A - \sum_{r=1}^{M-1} \frac{1}{r} (1-A)^r \right\},
\end{aligned} \tag{39}$$

where  $A = 2d_2 / [(M-1)d_1 + 2d_2]$ .

For  $q \geq 2$ , Gotelli and Chao [61] obtained

$${}^q\hat{D} = \left[ \sum_{m_i \geq q} \frac{m_i^{(q)}}{M^{(q)}} \right]^{1/(1-q)} \tag{40}$$

where  $x^{(j)} = x(x-1)\dots(x-j+1)$ . For example,  ${}^2\hat{D} = M(M-1) / \sum_{m_i \geq 2} m_i(m_i-1)$ , the inverse of Simpson's index without replacement (Eqs. 20 and 22).

The ill-conditioning of the inverse problems is particularly severe for the richness  ${}^0D$ . The general formula for an estimate of the system richness is

$${}^0\hat{D} = R(M) + \hat{d}_0, \tag{41}$$

and reduces to the unseen species problem for determining  $d_0$  [64, 65]. Since the sample size  $M$  and the richness  $R$  in the system are uncorrelated, rigorously, one must use information contained in the species fractions  $f_i$  or the clone counts  $c_k$  in the full system [66, 67]. However, a popular estimate for the system richness  $R(N)$  is the "Chao1" estimator [68, 61]

$$\text{Chao1} : \hat{R}(N) = R(M) + \frac{d_1^2}{2d_2}, \tag{42}$$

which is actually a lower bound and gives reliable estimates for systems of size only up to approximately double or triple the sample size  $M$ . The uncertainty of the Chao1 estimator has also been derived via a variance that is also a function of  $d_1$  and  $d_2$  [69]. The "Chao2" estimator gives the system richness as a function of measured incidence [61]

$$\text{Chao2} : \hat{R}(N) = R(M) + \frac{q_1^2}{2q_2}, \tag{43}$$

where  $q_1, q_2$  are the number of species found in 1 or 2 samples out of many (as in the  $1 \times M$  sampling method). Shen *et al.* [70] derived another estimate

$$\hat{R}(N) = R(M) + d_0 \left[ 1 - \left( 1 - \frac{d_1}{Md_0 + d_1} \right)^{N-M} \right], (44)$$

which is only reliable if the sample size  $M$  is more than half of the system size  $N$ . Many of these estimators have been coded into analysis software such as R and iNEXT [71].

Regardless of the estimator, the major limitation is an insufficient sample size  $M \ll N$ . Models predicting species abundances as a function of system size can help bridge this gap. For example a log-normal relationship for the clone count  $c_k$  [72] has been used to find agreeable results [73, 74]. In general, models can be extremely useful analyzing the effects of sampling, particularly when a Bayesian prior is desired.

We have outlined the basic mathematical frameworks for quantifying diversity that have utility across applications in different disciplines. The above summary of sampling assumes a “well-mixed” population, precluding any spatial dependence of the distribution of individual species. Spatially dependent sampling has been proposed for the origin of relationships between the number of species detected and the total area occupied by the population (see below). Below, we summarize a few modern applications in which the concepts of diversity are important and discuss the specific descriptions used in each field.

## 5. Fields in which diversity play a key role

### 5.1. Ecology, paradox of the plankton

The classic problem in the context of biological diversity is dubbed “the paradox of the plankton” and was originally discussed in a paper of the same title [75]. It describes diverse populations of plankton in environments of limited number of resources or nutrients. Sampled populations of plankton exhibit a large number of species even in low nutrient conditions during which one expects strong competition for resources. This observation runs counter to the “competitive exclusion principle” described in many settings [76].

Perhaps the most common application of diversity arises in biological population studies, specifically in ecology [6, 7, 8, 9, 10, 11]. Possible areas of application include the monitoring of ecosystems and the development of efficient species conservation strategies [2, 9, 30, 5, 31, 10, 29]. Multiple overlapping and nebulous definitions of ecological diversity have been advanced [27, 28, 25, 3, 4, 26, 29]. An early work by Fisher [6] introduced a logarithmic series model to mathematically describe empirical species diversity data. In this work, the notion of diversity index referred to a free parameter in the corresponding

model. In a later study, R. H. MacArthur [77] defined species diversity based on the size of the sampled area. In the ecological setting, multiple layers of subpopulations are an important feature of populations. These subpopulations may be delineated by another property of the individual species, such as size, weight, behavioral attributes, etc. Subpopulations can also be distinguished through their spatial distribution or occupation of different habitats. Whittaker [78, 79] qualitatively defined four types of diversity (point, alpha, beta, and gamma) conditioned on habitat or spatial distribution of the subpopulations [79]. Fundamentally, these differences arise from different methods of sampling, leading to different Hill numbers  ${}^qD$ . We summarize a few main descriptions below:

- “Point diversity” refers to samples taken at a single point or “microhabitat.” This quantity is typically operationally measured by trapping organisms at one or more specific points.
- “Alpha diversity” is defined as the diversity within an individual location or specific area. In general, one can define a Hill number derived from measurements at a specific location as  ${}^qD_\alpha$ , while the index  $\alpha \equiv {}^0D_\alpha$  is the richness encountered within a defined area or specific location. A few subtle variations in the definition of the index  $\alpha$  exist, mostly related to the sampling process [44, 45]. For example, in relation to beta diversity (discussed below), alpha diversity is the mean of the specific-location diversities across all locations within a larger landscape.
- “Gamma diversity” is the diversity index  ${}^qD_\gamma$  determined from the entire dataset, the total landscape, or entire ecosystem. The index  $\gamma \equiv {}^qD_\gamma$  typically denotes the total number of different species or clones at the largest scale. Note that the mean or sum of the alpha diversities is typically not equal to the gamma diversity. The nonlinearity of the Hill numbers as well as the intersection or exclusion of species amongst the different sites suggests a need for indices that connect alpha and gamma diversities.
- “Beta diversity” was devised to describe the difference in diversity between two habitats or between two different levels of ecosystems. While the different levels of diversity are designed to the spatial aspects of diversity, different “habitats” overlap, leading to some amount of arbitrariness in determining, or sampling of the  $\beta$ -diversity. Moreover, “beta diversity” was initially described in different ways [78, 79, 44], leading to confusion about its mathematical definition and use [47, 45, 44]. One possible definition is Whittaker’s [78]

multiplicative law  ${}^qD_\gamma \equiv {}^qD_\alpha {}^qD_\beta$  where here,  $\alpha$  is defined as the *mean* of the diversities across all micro-habitats. Whittaker’s definition describes “beta diversity”  ${}^qD_\beta = {}^qD_\gamma / {}^qD_\alpha$  as a measure to quantify the diversity in the total population relative to the mean diversity across all micro-habitats [44]. In the limit of  $q \rightarrow 1^-$ , we obtain the Shannon diversity relationship  $\text{Sh}_\gamma = \text{Sh}_\alpha + \text{Sh}_\beta$  according to Eq. (18). Another definition of  $\beta$  is given by Lande’s [80] additive law  $\gamma \equiv \alpha + \beta$  according to which diversity indices are measured in the same units. One concept associated with  $\beta$  in terms of the additive partitioning is species “turnover,” quantifying the difference in richness between the entire and the local population. As an example, consider two distinguishable or spatially separate habitats A and B. If A contains species  $\{a, b, c, d, e\}$  and B contains  $\{b, c, f, g\}$ , we find  $\beta_{\mathbf{A},\mathbf{B}} = 5$  associated with the set  $\{a, d, e, f, g\}$ . The laws of Whittaker and Lande sparked debates about how to properly define “beta diversity”, and led to the distinction between multiplicative and additive diversity measures [47, 45, 44].

- “Delta, Epsilon, Omega diversity” are other hierarchical definitions of diversities proposed by Whittaker [79]. Delta diversity is analogous to beta diversity but defined at the larger among-landscape scale, while epsilon diversity corresponds to gamma diversity, but at the “regional” scale that contains many “landscapes.” Omega diversity is measured at the biosphere scale, and thus characterizes the diversity of all ecosystems [81].
- “Zeta diversity” was introduced by Hui and McGeoch [82], and is defined by a set of  $\zeta$  indices to mathematically describe the species numbers between different partitions of a certain habitat. Specifically,  $\zeta_i$  is the mean number of species shared by  $i$  partitions. In particular,  $\zeta_1$  is the mean richness across all sites. For example, between two samples A and B or sets of data, the average number of species is  $\zeta_1 := (R_{\mathbf{A}} + R_{\mathbf{B}})/2$ , while the intersection is  $\zeta_2 := |\mathbf{A} \cap \mathbf{B}|$ . Generalizations to multiple samples can be defined using a series of zeta diversity indices  $\zeta_i$ .
- Many other indices have been defined for different applications. The Jaccard index [83, 78, 44, 82] is defined as  $J(\mathbf{A},\mathbf{B}) = |\mathbf{A} \cap \mathbf{B}|/|\mathbf{A} \cup \mathbf{B}|$ , and is a general measure for quantifying the similarity in richness between two sets of populations A and B. Margalef’s index [84] and Menhinick’s index [85] are relative richness measures given by  $R/\ln N$  and  $R/\sqrt{N}$ , respectively. Other indices include the Bray-Curtis dissimilarity [86], the Berger-Parker diversity index [87] as defined in

Eq. (24), Fager’s index [88], Keefe and Bergersen’s index [89], McIntosh’s index [90], and Patil and Taillie’s index [91].

The myriad of different definitions of indices have sprung from specific cases of the Hill number and the ideas of different spatial scales of ecosystems. There is potential to further unify these definitions in a more systematic way using mathematical norms and more general mathematical structures of spatial dispersal of particles.

### 5.2. Area-Species Law and Island Biodiversity

A particularly consistent, albeit qualitative feature observed in ecology is the species-area relationship (SAR) which relates the measured number of species (richness) with the relevant area. These areas can represent distinct habitats, such as mountain tops, or islands. For the latter, much work has been done in the subfield of island biodiversity.

The SAR is typically expressed as a power-law relationship between the number of species (or richness)  $R$  and the habitat/island area:

$$R = cA^z, \quad (45)$$

where  $c$  is a constant prefactor and  $z$  is an exponent. On a log-log plot,  $\log R = \log c + z \log A$  defines a line with slope  $z$ . An example of the area-species law for species counts of long-horned beetles in the Florida Keys is shown in Fig. 3, yielding a slope  $z = 0.29$ . An alternative species-area relationship is  $e^R = cA^z$  [92], which is a straight line on a semi-log plot.

The classic book by MacArthur and Wilson [93] and many subsequent analyses have promoted and extensively analyzed the SAR idea. In MacArthur and Wilson’s neutral equilibrium theory, immigration to and death on an island are monotonically decreasing and increasing functions of the number of species already on the island, respectively. Typically, measured values of the exponent fall in the range  $z \sim 0.1 - 0.4$ . Field work has also found relationships between the parameters  $c$  and  $z$  and system-specific attributes such as the island distance to the mainland, habitat type, etc [93, 95]. Nonetheless, reasonable predictions based on Eq. (45) are ubiquitous across many ecological examples.

Origins of the robustness of the SAR have been proposed [96, 97, 98]. Different models for species populations  $n_i$  or clone counts  $c_k$  were surveyed and the corresponding species-area laws were derived by He and Legendre [97]. Spatial clustering of species and the averaging of random measurements was shown to robustly generate a power-law species-area curve [97, 98], highlighting the fundamental importance of sampling.

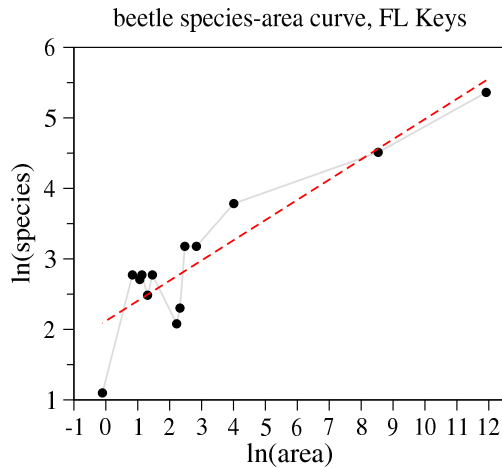


**Figure 3.** Plot of  $\ln R$  versus  $\ln A$  with area  $A$  measured in terms of  $\text{km}^2$ . Species counts of long-horned beetles in the Florida Keys are plotted against the island size [94]. The linear regression line yields a slope of  $z = 0.29$ . Typically, fits of the species-area exponent  $z$  yield a small number.

### 5.3. Gut Microbiome

One area of ecological system that has recently received much attention is the human microbiome, especially the gut. The bacterial ecosystem in the gut is important for health and can impact cardiovascular disease, diabetes, neuropsychiatric diseases, inflammatory bowel disease (IBD), digestive and metabolic function to the point that fecal transplantation (bacteriotherapy) has become an effective treatment for recurrent *C. difficile colitis* infections [100]. This type of infection often occurs after antibiotics disrupt the gut microbiome. Transplants have also shown to be effective in treating slow-transit constipation [101].

Recent efforts to collect and curate gut microbiome data have included NIH’s Human Microbiome Project (HMP) [102, 103] and the European Metagenomics of the Human Intestinal Tract (MetaHIT) [104, 105, 106], as well as the integration of the data in reference [107]. Each dataset contains sequence data from samples from different body regions of hundreds of individuals, both healthy and diseased.

Bacterial species are typically determined by sequencing of the 16S ribosomal RNA (rRNA), a component of prokaryotic ribosomes that contain hypervariable regions that are species-specific. However, closely related taxa can have very similar sequences, making separation imperfect [108]. Nonetheless, with numerous public databases [109, 110, 111, 99], estimates of species abundances in samples are readily available. In the gut, there are typically on the order of 1000 bacterial species, with Bacteroidetes and Firmicutes being the dominant phyla [112, 113]. Indeed, lower gut diversity is seen to be associated with conditions such as Crohn’s disease [112]. For example, the fre-

quency distribution of bacterial species in healthy and irritable bowel syndrome patients are shown in Fig. 4. The quantification of diversity of human microbiome is an essential step in ongoing research and the diversity indices have been applied to microbiome data, including  $\alpha$ -diversity and  $\beta$ -diversity across the microbiome from different anatomical regions and different patients. Similar to island biodiversity problem, the gut microbiome can be qualitatively modeled as birth-death-immigration (BDI) process.

### 5.4. Barcoding Experiments

Besides taxonomy of gut bacteria, the accurate identification of animal and plant species from samples is an essential task in ecology. In the early 2000’s a DNA barcoding method was developed to read relatively short DNA regions specific to certain species [117, 118]. These *barcodes* are typically found in mitochondrial DNA and often derived from a region in the cytochrome oxidase gene [117]. By sequencing samples and comparing with a sequence database such as The Barcode of Life Data System [119, 120], one can infer the number of species present within a sample. Detecting specific species within samples using DNA barcoding and DNA libraries have been used in many applications including identification of birds [118], identification of flowering plants [121], detecting contaminants [122], and tracking plant composition in processed foodstuffs [123].

Recently, a number of barcoding or tagging protocols [124, 125, 126] have been developed to genetically label a large population of cells to study how they differentiate and proliferate, especially in the context of hematopoiesis [127, 114, 128, 115, 129] and cancer progression [130, 131, 132]

A novel approach used to investigate hematopoiesis exploits *in situ* barcodes [127]. Mice were engineered with an enzyme (Sleeping Beauty Transposase) that randomly moves DNA sequences (transposons) to different parts of the genome. The transposase is designed to be controllable by doxycycline, an antibiotic that can be used to switch on or off gene regulation. When the transposase is briefly activated, transposons within cell are randomly rearranged within a brief period. Since the genome length  $\gg$  transposon length, the new locations of the transposons will be distinct across the “founder” cells. After switching off the transposase, proliferation of “founder” cells will impart, except for rare DNA replication events, the same genomic sequence to its daughter cells. These collections of cells constitute a multiclonal population that proliferates and differentiates.

Analysis of the clonal population within differentiated cell pools show that granulocytes derive from stem cells at particular time points during the life of

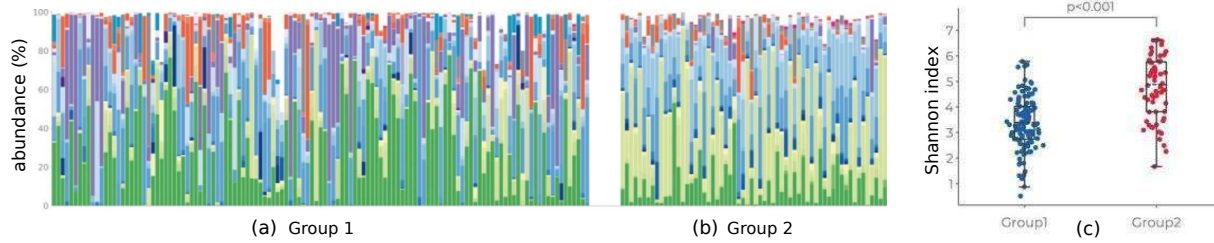


**Figure 4.** Frequencies of approximately 200 species of bacteria distributed across about a dozen phyla. (a) Group 1 depicts the relative abundance distribution for healthy individuals while (b) Group 2 shows the pattern for irritable bowel syndrome (IBD) patients. The differences in abundance patterns are apparent and have been quantified using the Shannon index for each individual plotted in (c). From Park *et al.* [99].

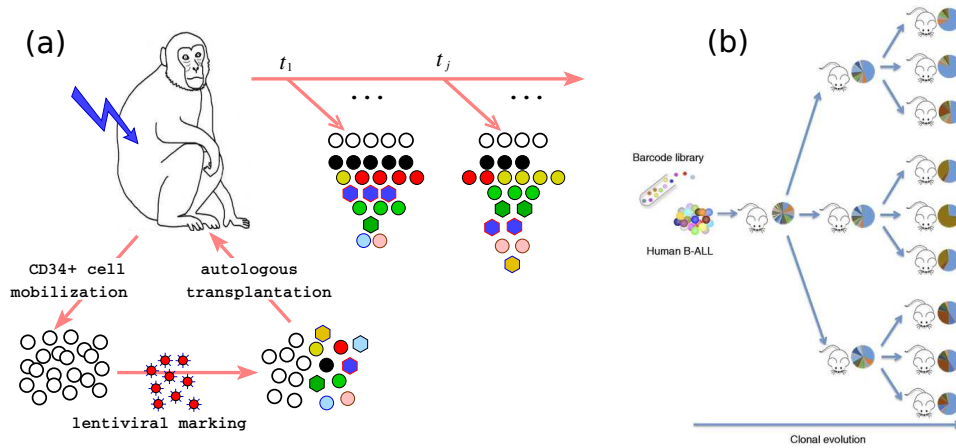


**Figure 5.** (a) Protocol for Viral Integration site (VIS) barcoding studies of hematopoiesis in rhesus macaque [114, 115, 52]. Here, “barcodes” are defined by the random integration sites of a lentiviral vector. (b) Xenograft barcode experiments using mice [116] in which a library of barcodes was used to tag leukemia-propagating cells before direct transplantation into mice.

the mouse [127]. Comparing clonal abundance structure within different cell lineages showed that clones originally predominant in the lymphoid lineages eventually arise in myeloid cells, indicating that multipotent progenitor cells continually produce cells of both lineages. These conclusions arise after statistical analysis of the clone (defined by their transposon sites) abundance distribution within different groups of cells.

In another recent series of studies on hematopoiesis, stem cells (HSCs) were extracted from rhesus macaques and infected with a lentiviral vector. The lentivirus integrates its short genome randomly and uniquely in the genome of the HSCs. The infected stem cells are autologously transplanted into the animal and some of them resume differentiation into progenitor cells that transiently proliferate and further differentiate. Descendant cells carry the same genetic sequence, including the lentivirus integration locations, or the viral integration sites (VIS). Another approach is to use libraries of synthesized DNA/RNA as tags. Here, the different sequences, rather than their integration sites, serve as the distinguishing feature. This process avoids the need to determine viral integration sites (VIS).

In all the above approaches, each successive

generation of cells will acquire the same tag, viral integration site (VIS) or specific DNA barcode sequence, as their parent and ultimately the founder HSC. Compared to the Sleeping Beauty Transposon protocol, the VIS or barcoding experiments require an additional viral transfection step. Nonetheless, these VIS and barcoding experiments are equally effective in dissecting the differentiation process and quantifying lineage bias with age. For example, the variation (in time) of the abundances of a clone across different lineages indicates the level of fate switching of a stem cell [114, 133].

These experiments also enabled observation of biological mechanisms on a finer scale compared to traditional studies, allowing inference of parameters that are difficult to measure directly such as the initial HSC differentiation rate and the proliferative potential (number of generations) accessible to progenitor cells [52, 134].

After sampling, PCR amplification, and sequencing (each process exhibiting their specific errors), the relative species populations and clone counts within defined cell types can be quantified. Fig. 6(a) shows frequencies of barcode  $i$  as a function of sampling times

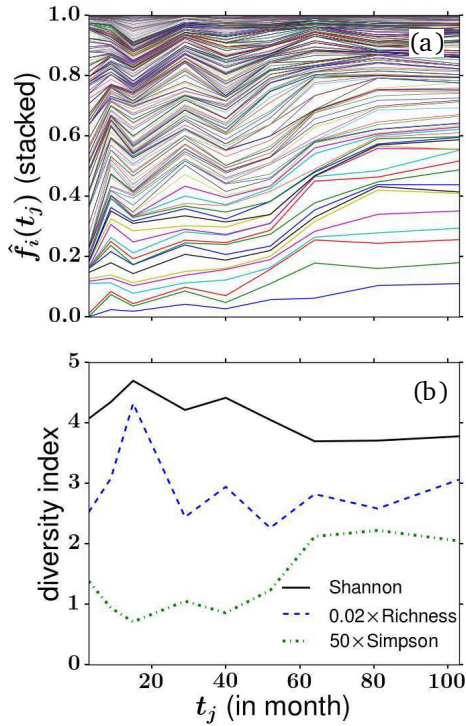


**Figure 6.** (a) The fractional populations of the largest clones (barcodes) detected in granulocyte blood samples from rhesus macaque. Relative populations are described by the distances between neighboring curves. (b) Diversity indices derived from the data in (a). The Simpson’s index and Shannon diversity are rescaled to fit on the same plot.

$t_j$  in rhesus macaque. The fraction of each clone is depicted by the vertical distance between two neighboring curves. Here, it is important to note that the “diversity” is a measure of the distribution of clone ID (barcodes) instead of lineages (cell types). In Fig. 6(b), we plot three different and rescaled diversity indices associated with the data in (a). The sampled richness is initially low at month 3 when barcoded clones have not fully differentiated and emerged in the peripheral blood. The sampled richness then peaks at month 9 before stabilizing after month 29. Simpson’s diversity seems to continue to increase after month 29 which may indicate more unevenness and coarsening (fewer clones dominating the total population). Shannon’s index is shown to decrease slightly, suggesting a decrease in the effective number of barcodes.

Sun *et al.* [127] and Kim *et al.* [114] also used simple clustering algorithms that identified similar clones according to their activity patterns across time. They identified distinct groups of clones that are featured by different time points of contribution to hematopoiesis. Koelle *et al.* [133] calculated Shannon diversity to ensure comparability between animals, different cell types, and across time.

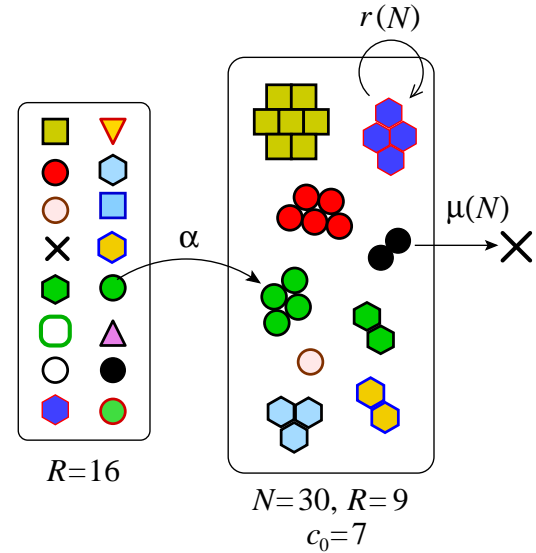


**Figure 7.** A simple multispecies birth-death-immigration (BDI) process [52, 134, 135, 136]. A constant “source” (*i.e.*, stem cells with slow dynamics) of 16 cells, each of a different clone, undergo asymmetric differentiation with rate  $\alpha$  to produce differentiated cells that can undergo birth or death with rates  $r(N)$  and  $\mu(N)$  that may depend on the total population in the differentiated pool. In this example, the differentiated population contains  $N = 30$  cells,  $R = 9$  different clones (barcodes), thus leaving  $c_0 = 7$  unseen species.

The employment of neutral barcodes to study blood cell populations is statistically insensitive to spatial partitioning (different tissues in the organism). Nonetheless, small sampling  $M \ll N$  makes inference difficult. Thus, mechanistic simplifications and mathematical models have been used to quantify clonal evolution. Assuming a multispecies birth-death-immigration process (Fig. 7) Dessalles *et al.* [135] found explicit steady-state distribution functions for  $n_i$  (log series) and  $c_k$  (Poisson) for constant  $r$  and  $\mu$ , as well as formulae for the expected Shannon’s and Simpson’s diversities. Goyal *et al.* [52] derived a master equation for the evolution of  $\mathbb{E}[c_k]$  and then extended the solution to expected clone counts in the progenitor cell and sampled cell pools. By comparing results to the expected clone count in the sample at steady-state, they were able to infer kinetic parameters of the differentiation process. Biasco *et al.* [137] proposed two candidate stochastic models for  $n_i$  and used Bayesian Information Criterion (BIC) to assess the likelihood of each.

### 5.5. Immunology

Another intra-organism system for which diversity plays a key functional role is the adaptive immune system in vertebrates. The simplest immune subsystem consists of lymphoid cells and tissues. T cells originate from hematopoietic stem cells and

develop in the thymus. During development, a T cell's receptor sequence is chosen before a *naive* T cell is exported to the peripheral tissues (blood and lymph nodes). Each T cell in the body contains one type of receptor that binds to specific antigens and self-antigens in the body. Antigens are strands of amino acids presented on the surface of Antigen-Presenting cells (APCs). Naive T cells (those that have not previously strongly interacted with antigen) can be activated through association of the surface T cell receptors (TCRs) with antigens presented by major histocompatibility complex (MHC) molecules on the surface of APCs.

Since the space of antigens (the different amino acid sequences, or epitopes, presented by MHCs) is astronomically large, a large number of different TCR sequences should be present in the organism in order to mount an effective response to a wide range of infections. However, as each T cell matures in the thymus, they express only one TCR type, or clonotype. TCRs are typically composed of a dimer, an alpha chain and a beta chain. During T cell development and TCR generation, gene segments of the alpha chain and beta chain, called VJ and VDJ segments, respectively, undergo random recombination. During development, one of two different diverse (D) regions of thymocytes recombine with one of six different joining (J) regions first, followed by rearrangement of the variable (V) region connecting it to the now-combined DJ segment. During this recombination, many different deletions and splicings can also occur leading to many different variants of the gene and TCR protein sequences.

The number of different possible genes for the alpha chain and the beta chain are essentially multiplied because the functional moiety of the TCR is a heterodimer of the alpha and beta chain. Estimates of the total possible number of clones is  $R > 10^{15}$  [138, 139]. However, before export, a complex selection process occurs [140]. Positive selection eliminates T cells that interact too weakly with MHC molecules. Subsequently, negative selection eliminates those T cells and TCRs that bind too strongly to epitopes. Cells that escape negative selection may lead to autoimmune disease as they react to self-proteins.

T cells expressing the same TCR in the periphery constitute an "immunoclone" or "immunotype." The total number of different distinct immunoclones realized in an organism (the richness) defines its T cell repertoire and is estimated to range from  $10^6 - 10^8$  [141], with the lower range describing mice and the higher range an estimate for man. T cell diversity is an important factor in health. For example, it has been shown to influence the tumor microenvironment and survival in lymphoma [142].

Although specific TCR sequences  $i$  can be

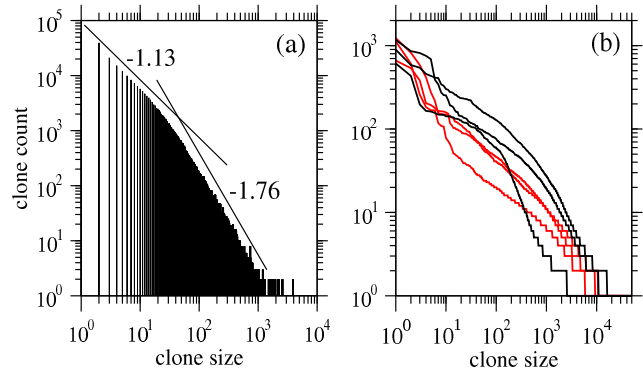


**Figure 8.** Examples of recently published clone count data. (a) Clone counts derived from a small sample ( $10^5$  sequences) of B and T cells [139]. Note the broad distribution described by a biphasic power-law curve. Ignoring the largest clones, power-law fits for each regime yield slopes of  $-1.13$  and  $-1.76$ . (b) Human TCR clone counts for three HIV-infected (red) and three uninfected (black) individuals show qualitative differences between the distributions (unpublished). Other data from mice and humans, under different conditions and in different cell types, have been recently published [143, 144].

determined, and their populations  $n_i$  measured and estimated, the TCR identities vary significantly across individuals (private sequences) so clone counts are typically studied. Fig. 8(a) shows T cell clone counts  $d_k$  sampled from mice [139] that exhibit a biphasic power-law behavior. Fig. 8(b) shows preliminary clone counts for six individuals, three HIV-negative patients and three HIV-infected patients [145].

Quantifying T cell diversity is confounded by a number of technical limitations. The complete T cell repertoire in an animal cannot typically be directly measured. Rather, as in most other applications, small samples of the entire population are usually drawn. In blood draws in humans, perhaps only  $0.1 - 1\%$  of the blood is drawn and sequenced. Thus, clones that have small populations may be missed in the sample. Besides sampling, sequencing requires PCR amplification of the sample, leading to PCR bias, especially in the larger-sized clones. Finally, as in many other applications, there are multiple subclasses of the T cell population. Naive T cells that are activated by antigens develop into memory T cells that carry the same TCR and that can further proliferate. Thus, it is difficult to separate the clone counts of different subpopulations such as naive or memory T cells.

Many mathematical models for the development and maintenance of the immune systems have been developed [140, 138, 146, 135, 134, 147]. For the multiclonal naive T cell population, rudimentary insights can also be gleaned from a birth-death-immigration process, much as in the modeling of hematopoiesis. Here, the thymus mediates the immigration of a large number of clones, which undergo

homeostatic proliferation and death in the periphery. Immigration rates can be different for different clones, depending on the likelihood of specific recombination patterns [148, 149]. Proliferation in the periphery depends on interactions between self-peptides with T cell receptors and is thus clone-dependent. Recently, it has been shown that TCR-dependent thymic output and proliferation rates (a nonneutral BDI model) influence the measured clone count patterns [150]. These processes form and maintain a diverse T cell receptor repertoire, which is typically characterized by its richness. Unlike the barcode abundances arising during hematopoiesis, the neutral BDI processes are not able to capture the shapes of the measured TCR clone counts.

It is also known that T cell residence times depend on interactions between tissues and T cell receptors. Thus, different clones of T cells are expected to be differentially spatially distributed in the body. Hence, diversity metrics should be defined within and between “habitats,” much like that in ecology.

Finally, it is known that T cell richness decreases with age [151, 152, 153, 154]. Qualitatively, a loss of diversity has been predicted within the multispecies birth-death-immigration process by assuming a decreasing thymic output rate with age. Even when the thymus is completely shut down, the diversity of the T cell repertoire slowly decreases as successive clones go extinct and the clone abundance distribution “coarsens.” In humans, since the overall T cell population is primarily maintained by proliferation rather than thymic immigration [155], the reduction in diversity is a slow process.

### 5.6. Societal Applications of Diversity: Wealth distributions

Concepts of diversity have been naturally applied in human social contexts [21, 19, 20, 156], including physical, cultural, educational [32, 24], and economic settings. For example, the distribution of wealth is the chief metric in many economic and political studies. As with all applications, data collection, sampling and delineating differences in attributes are key challenges.

Wealth or income, unlike species, are essentially continuous and ordered quantities, and can be described by many indices designed by economists to measure different wealth attributes of a population. Distinct from cellular or ecological contexts, socioeconomic diversity is often also discussed in terms of “inequality,” “evenness,” or “polarization.” Diversity or “inequality” indices in the socioeconomic setting typically assume a number of additional concepts including

- Individual identities are irrelevant. This is

analogous to barcoding studies of a singular cell type in which the barcode identity is not important.

- Size and total wealth invariance: The diversity is invariant to the total population size. Only proportions of the total population that are associated with a proportion of the total wealth are relevant.
- Dalton principle: Any inequality index should increase if any amount of wealth is transferred from an entity to one with higher existing wealth.

Mathematically, one starts by ordering the wealth or income of a population of  $N$  entities  $w_1 \leq w_2 \dots \leq w_i \leq w_{i+1}, \dots \leq w_N$ . For large  $N$ , the rescaled wealth distribution  $w(f) \equiv w_{fN}$  is a function of the relative fraction of the total population  $f = n/N \in [0, 1]$ . Furthermore, we can define a normalized wealth distribution or density

$$\tilde{w}(f) = \frac{w(f)}{W_T}, \quad W_T = \sum_{i=1}^N w_i \approx \int_0^1 w(f') df', \quad (46)$$

and the corresponding cumulative distribution

$$W_i = \frac{1}{W_T} \sum_{j=1}^i w_j \quad (47)$$

or

$$W(f) = \int_0^f \tilde{w}(f') df' \equiv \frac{1}{W_T} \int_0^f w(f') df'. \quad (48)$$

The functions  $W(f)$  are known as “Lorenz-consistent [33]” if they satisfy the above conditions. Four representative Lorenz consistent raw wealth distributions are shown in Fig. 9(a) as functions of the individual index. In Fig. 9(b), we plot the continuous cumulative rescaled wealth distribution  $W(f)$  as a function of the relative population fraction  $f$  corresponding to the wealth distributions shown in Fig. 9(a). From any ordered distribution, we can define a so-called “Lorenz curve” that illustrates many indices graphically. The Lorenz curve is defined as the cumulative wealth of all individuals of a relative index  $f = n/N$  and lower.

Many indices can be visualized by the Lorenz curves. For example, the Gini index [157, 158] for the red distribution (linear wealth) in Fig. 9(a) is calculated by the area of the red shaded region ( $A$ ) divided by the area under the equality curve ( $A + B = 1/2$ ):  $\text{Gini} = A/(A+B) = 2A$ . In a society where every person receives the same income, the Gini index equals zero. However, if the total wealth is concentrated in only one out of  $N$  entities,  $\text{Gini} = 1 - 2/N$ . This motivates to define the Gini index for discrete cumulative wealth values  $W_i$  according to

$$\text{Gini} = 1 - \frac{2}{N} \sum_{i=1}^N W_i, \quad (49)$$

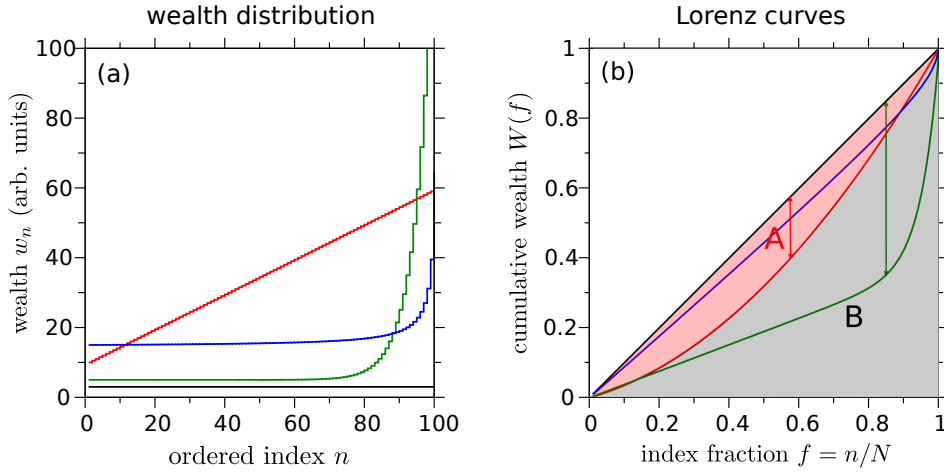


**Figure 9.** (a) Ordering of all  $N = 100$  individuals in increasing wealth or income. The hypothetical wealth distributions plotted are  $w_i = 3$  (equal wealth, black curve),  $w_i = 10 + (i - 1)/2$  (linear distribution, red),  $w_i = 5 + e^{i/5-15} - e^{-14.8}$  (green), and  $w_i = 14.5 + 50/(101 - i)$  (blue). The latter three represent distributions with some amount of inequity. (b) These inequalities can be visually quantified by their corresponding Lorenz curves, plotted as the relative fraction of the population  $f$ . The Lorenz curve for a perfectly uniform wealth distribution is given by the straight diagonal line. The area between the diagonal equality line and any other Lorenz curve can be used to visualize the Gini coefficient of the associated wealth distribution. The Gini coefficient is calculated by dividing the difference in areas between the equality line and the Lorenz curve in question ( $A$ ) by the total area ( $A + B = 1/2$ ) under the equality curves:  $\text{Gini} = A/(A + B)$ . The “Robin Hood” index is defined as the maximum difference between the equality line and a given Lorenz curve, and are indicated by arrows for the red and green curves.

while the “Hoover” or “Robin Hood” index defined by [34, 159, 160]

$$H = \max_f \{|f - W(f)|\} \quad (50)$$

is the Legendre transform at  $f^*$ , the fraction of individuals corresponding to  $dW(f)/df|_{f=f^*} = 1$ . For the two Lorenz curves in Fig. 9(b), the Robin Hood index is indicated by the two corresponding arrows.

The Robin Hood index happens to be a specific case of the Kolmogorov-Smirnoff statistic as defined in Eq. (12) for two cumulative distributions. For convex functions  $W(f)$  such that  $W(0) = 0$ ,  $W(1) = 1$ , the index  $H$  corresponds to the fraction of the total wealth that needs to be distributed in order to achieve uniform wealth. This can be seen by considering the wealths  $w_i$  up to an index  $n^*$  such that  $w_i \leq N^{-1}$  for all  $i \leq n^*$ . The total wealth that needs to be redistributed to obtain equal wealth fractions  $N^{-1}$  for every individual is

$$H = \sum_{i=1}^{n^*} \left( \frac{1}{N} - w_i \right) = \frac{n^*}{N} - W_{n^*} \approx f^* - W(f^*). \quad (51)$$

Another possibility is to sum over all entities  $w_i$  according to

$$\begin{aligned} H &= \frac{1}{2} \sum_{i=1}^N \left| \frac{1}{N} - w_i \right| \\ &\approx \frac{1}{2} \int_0^1 |1 - w(f)| df \\ &= \frac{1}{2} \left[ \int_0^{f^*} (1 - w(f)) df + \int_{f^*}^1 (w(f) - 1) df \right] \end{aligned}$$

$$= f^* - W(f^*). \quad (52)$$

The specific redistribution is not specified but is related to mathematical concepts of optimal transport and the Wasserstein distance.

Moreover, it is possible to quantify inequity according to the Theil index [161, 162, 163]

$$T = \frac{1}{N} \sum_{i=1}^N \frac{w_i}{\mathbb{E}[w]} \log \left( \frac{w_i}{\mathbb{E}[w]} \right), \quad (53)$$

which corresponds to a relative entropy as defined in Eq. (8). In this case, the entropy of the distribution of  $w_i$  is measured with respect to the expectation value  $\mathbb{E}[w] = N^{-1} \sum_{i=1}^N w_i$ . If  $\sum_{i=1}^N w_i = 1$ , we may interpret  $w_i$  as the probability of finding an individual in income class  $i$ , and  $\mathbb{E}[w] = N^{-1}$  corresponds to the relative share of equally distributed wealth.

These indices do not impart any opinion and may not capture typical social concepts. In an effort to better quantify concepts such as inequity or “polarization,” a number of polarization indices have been proposed to be more directly correlated with social tension and unrest. For example, Esteban and Ray [35, 36] developed a measure of polarization to account for clusters within which individuals are more similar in an attribute  $x$  (such as wealth) that they are between clusters. While there may be many ways to define polarization, imposing a few reasonable features and constraints can narrow down the allowable forms. First, they assume an “identity-alienation framework” in which an individual also identifies with his own distribution  $f(x)$  at value  $x$ . An effective “antagonism”

of an individual with attribute  $x$  towards those with attribute  $y$  is defined as  $T[f(x), d]$  where a simple form for the distance is  $d = |x - y|$ . The polarization  $P$  is then assumed to take the form

$$P[f] = \int \int T[f(x), |x - y|] f(x) f(y) dx dy. \quad (54)$$

By imposing axioms that the polarization (i) cannot increase if the distribution is “squeezed” (compressed towards its peak), (ii) must increase if two non-overlapping distributions are moved farther apart, and (iii) the polarization should be invariant to scalings of the total population. Using these constraints, the polarization can be more explicitly defined as

$$P[f] = \int \int f^{1+\alpha}(x) f(y) |x - y| dx dy, \quad (55)$$

where  $1/4 \leq \alpha \leq 1$  describes the identification to the population exhibiting ones attribute (polarization sensitivity). Note that when  $\alpha = 0$ , the form of  $P[f]$  resembles the total potential energy of a system of particles which is distributed according to  $f(x)$  and exhibits an interaction energy  $|x - y|$ . The discrete analogue of Eq. (55) is  $P[f] \propto \sum_{i,j} f_i^{1+\alpha} f_j |x_i - x_j|$ , for which the individuals  $i, j$  can be generalized to groups. In empirical studies, the Esteban and Ray polarization measure is given by

$$P_{ER}[f] \propto \sum_{i,j} \pi_i^{1+\alpha} \pi_j |\mu_i - \mu_j|, \quad (56)$$

where

$$\pi_i = \int_{x_{i-1}}^{x_i} f(x) dx \quad \text{and} \quad \mu_i = \frac{1}{\pi_i} \int_{x_{i-1}}^{x_i} x f(x) dx, \quad (57)$$

are the relative frequency and the mean of the wealth in group  $i$ , respectively [164]. D’Ambrosio and Wolff suggested suggested to replace the difference of mean wealths in Eq. (56) by the Kolmogorov measure of variation distance [164, 165]

$$\text{Kov}_{ij} = \frac{1}{2} \int |f_i(y) - f_j(y)| dy \quad (58)$$

to obtain

$$P_{DW}[f] \propto \sum_{i,j} \pi_i^{1+\alpha} \pi_j \text{Kov}_{ij}. \quad (59)$$

Additional indices have been proposed, including a class of polarizations by Tsui and Wang [166] of the form

$$P_{TW}(\mathbf{x}) = \frac{1}{N} \sum_{i=1}^N \psi(d_i), \quad d_i = \left| \frac{x_i - m(\mathbf{x})}{m(\mathbf{x})} \right|, \quad (60)$$

where  $\psi$  is a smooth function of the rescaled distance  $d_i$ . The median income  $m(\mathbf{x})$  is computed from the individual incomes  $x_i$  ( $1 \leq i \leq N$ ).

Many of these polarization metrics can in fact be expressed in terms of the Gini coefficient. For

example, the Foster–Wolfson polarization index is defined as [167]

$$P_{FW}(\mathbf{x}) = (\text{Gini}_B - \text{Gini}_W)(\mu(\mathbf{x})/m(\mathbf{x})), \quad (61)$$

where  $\mu(\mathbf{x})$  is the corresponding mean income, and the subscript indices  $B$  and  $W$  denote the between and within group Gini coefficients. According to the definition of  $P_{FW}(\mathbf{x})$ , inequity differs from polarization in the following way: The Gini index as the sum of  $\text{Gini}_B$  and  $\text{Gini}_W$  quantifies the unequal distribution of wealth in a society whereas polarization is measured in terms of the difference of  $\text{Gini}_B$  and  $\text{Gini}_W$ . Thus, an increase in within-group inequality leads to a larger total inequality, but to a lower polarization. A more refined understanding or socioeconomic diversity will need to consider multiple classes of attributes, including possible geographic or spatial distributions.

The described polarization measures are relevant not only in the context of wealth distributions, but they are also able to provide important insights in other sociological phenomena associated with the notion of diversity. As one example, quantitative measures of polarization are applicable to examine factors that influence the cohesiveness of groups [23]. In addition, diversity measures may help to identify mechanisms which lead to inequality among different social groups in our education system [24]. In this context, the social entropy theory aims to quantitatively compare the diversity across social systems such as societies, organizations, and individual groups [19, 168, 20].

## 6. Summary and Discussion

In this review, we provided an overview of the most relevant measures of diversity and their information-theoretic counterparts. We summarized common applications of diversity indices in biological and ecological systems. Despite the ambiguity in the definitions and the variety of different diversity measures [27, 28, 25, 3, 4, 26, 29], the concept is of great importance for the monitoring of ecosystems and in the context of conservation planning [2, 9, 30, 5, 31, 10, 29].

We also described the importance of a quantitative treatment of diversity for experiments in the study of the gut microbiome, stem cell barcoding, and the adaptive immune system. Finally, we discussed examples of the application of diversity measures in human social systems including the characterization of wealth distributions in societies and measures of political or cultural polarization. Scientific conclusion in these fields, and in ecology, are particularly sensitive to sampling and measurements. However, accurate measurements [169], meaningful classification, spatial resolution [98], and informative sampling protocols [66, 73] remain elusive across almost all fields.

## 7. Acknowledgments

This work was supported in part by grants from the NSF through grant DMS-1814364, the Army Research Office through grant W911NF-18-1-0345, and the National Institutes of Health through grant R01HL146552. The authors also thank Greg Huber for insightful discussions.

## References

- [1] Nei M 1973 *Proceedings of the National Academy of Sciences* **70** 3321–3323
- [2] Heywood V H, Watson R T *et al.* 1995 *Global biodiversity assessment* vol 1140 (Cambridge University Press Cambridge)
- [3] Purvis A and Hector A 2000 *Nature* **405** 212
- [4] Whittaker R J, Willis K J and Field R 2001 *Journal of Biogeography* **28** 453–470
- [5] Sala O E, Chapin F S, Armesto J J, Berlow E, Bloomfield J, Dirzo R, Huber-Sanwald E, Huenneke L F, Jackson R B, Kinzig A *et al.* 2000 *science* **287** 1770–1774
- [6] Fisher R A, Corbet A S and Williams C B 1943 *The Journal of Animal Ecology* 42–58
- [7] Magurran A E 1988 *Ecological diversity and its measurement* (Princeton university press)
- [8] Benton M J 1995 *Science* **268** 52–58
- [9] Courtillot V and Gaudemer Y 1996 *Nature* **381** 146
- [10] Alroy J 2004 *Evolutionary Ecology Research* **6** 1–32
- [11] Stollmeier F, Geisel T and Nagler J 2014 *Physical review letters* **112** 228101
- [12] Blume M E, Crockett J and Friend I 1974 *Survey of Current business* **54** 16–40
- [13] Blume M E and Friend I 1975 *The Journal of Finance* **30** 585–603
- [14] Rajan R, Servaes H and Zingales L 2000 *The journal of Finance* **55** 35–80
- [15] Goetzmann W N and Kumar A 2008 *Review of Finance* **12** 433–463
- [16] Haldane A G and May R M 2011 *Nature* **469** 351
- [17] Greenberg J H 1956 *Language* **32** 109–115
- [18] Yule C U 2014 *The statistical study of literary vocabulary* (Cambridge University Press)
- [19] Bailey K D 1990 *Social entropy theory* (SUNY Press)
- [20] Balch T 2000 *Autonomous robots* **8** 209–238
- [21] Neckerman K M and Torche F 2007 *Annu. Rev. Sociol.* **33** 335–357
- [22] Ostrom E 2009 *Understanding institutional diversity* (Princeton university press)
- [23] Mäs M, Flache A, Takács K and Jehn K A 2013 *Organization science* **24** 716–736
- [24] Domina T, Penner A and Penner E 2017 *Annual Review of Sociology* **43** 311–330
- [25] Sepkoski J J 1988 *Paleobiology* **14** 221–234
- [26] Ricotta C 2005 *Acta biotheoretica* **53** 29–38
- [27] Simpson E H 1949 *Nature* **163** 688
- [28] Hurlbert S H 1971 *Ecology* **52** 577–586
- [29] Sarkar S 2006 *Acta Biotheoretica* **54** 133–140
- [30] John Sepkoski Jr J 1998 *Philosophical Transactions of the Royal Society of London. Series B: Biological Sciences* **353** 315–326
- [31] Margules C R and Pressey R L 2000 *Nature* **405** 243
- [32] Herrnstein R J and Murray C 1994 *The Bell Curve* (Free Press)
- [33] Lorenz M O 1905 *Publications of the American Statistical Association* **9** 209–219
- [34] Edgar Malone Hoover J 1936 *Review of Economics and Statistics* **18** 162–171
- [35] Esteban J M and Ray D 1994 *Econometrica* **62** 819–851
- [36] Duclos J Y, Esteban J and Ray D 2004 *Econometrica* **72** 1737–1772
- [37] Grubb M, Butler L and Twomey P 2006 *Energy policy* **34** 4050–4062
- [38] Cover T M and Thomas J A 2012 *Elements of information theory* (John Wiley & Sons)
- [39] Jaynes E T 1963 *Information Theory and Statistical Mechanics Statistical Physics* ed Ford K (Benjamin, New York) p 181
- [40] Spellerberg I F and Fedor P J 2003 *Global ecology and biogeography* **12** 177–179
- [41] Lin J 1991 *IEEE Transactions on Information theory* **37** 145–151
- [42] Hill M O 1973 *Ecology* **54** 427–432
- [43] Tuomisto H 2010 *Oecologia* **164** 853–860
- [44] Tuomisto H 2010 *Ecography* **33** 2–22
- [45] Jost L 2007 *Ecology* **88** 2427–2439
- [46] Rényi A *et al.* 1961 On measures of entropy and information *Proceedings of the Fourth Berkeley Symposium on Mathematical Statistics and Probability, Volume 1: Contributions to the Theory of Statistics* (The Regents of the University of California)
- [47] Jost L 2006 *Oikos* **113** 363–375
- [48] Heip C 1974 *Journal of the Marine Biological Association of the United Kingdom* **54** 555–557
- [49] Wattis J A D and King J R 1998 *Journal of Physics A* **31** 7169
- [50] DOrsogna M R, Lakatos G and Chou T 2012 *The Journal of Chemical Physics* **136** 084110
- [51] DOrsogna M R, Lei Q and Chou T 2015 *Journal of Chemical Physics* **139** 014112
- [52] Goyal S, Kim S, Chen I S Y and Chou T 2015 *BMC Biology* **13** 85
- [53] Villela D A M, Garcia G d A and Maciel-de Freitas R 2017 *PLoS Neglected Tropical Diseases* **11** 1–20
- [54] Epopa P S, Millogo A A, Collins C M, North A, Tripet F, Benedict M Q and Diabate A 2017 *Parasites & vectors* **10** 376
- [55] Cianci D, Broek J V D, Caputo B, Marini F, Torre A D, Heesterbeek H and Hartemink N 2013 *Journal of Medical Entomology* **50** 533–542
- [56] Fisher R A, Corbet A S and Williams C B 1943 *The Journal of Animal Ecology* **12** 42–58
- [57] Bunge J and Fitzpatrick M 1993 *Journal of the American Statistical Association* **88** 364–373
- [58] Hsieh T and Chao A 2016 *Systematic Biology* **66** 100–111
- [59] Cox K D, Black M J, Filip N, Miller M R, Mohns K, Mortimor J, Freitas T R, Greiter Loerzer R, Gerwing T G, Juanes F and Dudas S E 2017 *Ecology and Evolution* **7** 11213–11226
- [60] Budka A, Lacka A and Szoszkiewicz K 2019 *Biodiversity and Conservation* **28** 385–400
- [61] Gotelli N J and Chao A 2013 Measuring and estimating species richness, species diversity, and biotic similarity from sampling data *Encyclopedia of Biodiversity* vol 5 (Academic Press) pp 195–211
- [62] Chao A, Gotelli N J, Hsieh T, Sander E L, Ma K, Colwell R K and Ellison A M 2014 *Ecological monographs* **84** 45–67
- [63] Chao A, Wang Y and Jost L 2013 *Methods in Ecology and Evolution* **4** 1091–1100
- [64] Efron B and Thisted R 1976 *Biometrika* **63** 435–447
- [65] Orłitsky A, Suresh A T and Wu Y 2016 *Proceedings of the National Academy of Sciences* **113** 13283–13288
- [66] Willis A and Bunge J 2015 *Biometrics* **71** 1042–1049
- [67] Willis A 2016 *Proceedings of the National Academy of Sciences* **113** E5096–E5096

- [68] Chao A 1984 *Scandinavian Journal of statistics* 265–270
- [69] Chao A 1987 *Biometrics* 783–791
- [70] Shen T J, Chao A and Lin C F 2003 *Ecology* **84** 798–804
- [71] Hsieh T, Ma K and Chao A 2016 *Methods in Ecology and Evolution* **7** 1451–1456
- [72] Curtis T P, Sloan W T and Scannell J W 2002 *Proceedings of the National Academy of Sciences* **99** 10494–10499
- [73] Locey K J and Lennon J T 2016 *Proceedings of the National Academy of Sciences* **113** 5970–5975
- [74] Locey K J and Lennon J T 2016 *Proceedings of the National Academy of Sciences* **113** E5097–E5097
- [75] Hutchinson G E 1961 *The American Naturalist* **95** 137–145
- [76] Hardin G 1960 *science* **131** 1292–1297
- [77] MacArthur R H 1965 *Biological Reviews* **40** 510–533
- [78] Whittaker R H 1960 *Ecological Monographs* **30** 279–338
- [79] Whittaker R H 1977 *Evolutional Biology* **10** 1–67
- [80] Lande R 1996 *Oikos* 5–13
- [81] Contoli L and Luiselli L 2015 *Web Ecology* **15** 33–37
- [82] Hui C and McGeoch M A 2014 *American Naturalist* **184** 684–694
- [83] Jaccard P 1900 *Bull Soc Vaudoise Sci Nat* **36** 87–130
- [84] Margalef D R 1957 *Memorias de la Real Academica de ciencias y artes de Barcelona* **32** 374–559
- [85] Menhinick E F 1964 *Ecology* **45** 859–861
- [86] Bray J and Curtis J 1957 An ordination of upland forest communities of southern Wisconsin.-ecological Monographs
- [87] Berger W H and Parker F L 1970 *Science* **168** 1345–1347
- [88] Fager E W 1957 *Ecology* **38** 586–595
- [89] Keefe T J and Bergersen E P 1977 *Water Research* **11** 689–691
- [90] McIntosh R P 1967 *Ecology* **48** 392–404
- [91] Patil G and Taillie C 1982 *Journal of the American statistical Association* **77** 548–561
- [92] Gleason H A 1922 *Ecology* **3** 158–162
- [93] MacArthur R and Wilson E O 1967 *The Theory of Island Biogeography* (Princeton University Press: Princeton, NJ)
- [94] Browne J and Peck S B 1996 *Canadian Journal of Zoology* **74** 2154–2169
- [95] Volkov I, Banavar J R, Hubbell S P and Maritan A 2003 *Nature* **424** 1035–1037
- [96] Connor E F and McCoy E D 1979 *American Naturalist* **113** 791–833
- [97] He F and Legendre P 2002 *Ecology* **83** 1185–1198
- [98] Martín H G and Goldenfeld N 2006 *Proceedings of the National Academy of Sciences* **103** 10310–10315
- [99] Park S Y, Nanda S, Faraci G, Park Y and Lee H Y 2019 *Journal of Biomedical Informatics: X* **2** 100040
- [100] Wilson B C, Vatanen T, Cutfield W S and O’Sullivan J M 2019 *Frontiers in Cellular and Infection Microbiology* **9** 2
- [101] Tian H, Ge X, Nie Y, Yang L, Ding C, McFarland L V, Zhang X, Chen Q, Gong J and Li N 2017 *PLoS ONE* **12** e0171308
- [102] 2014 *Cell Host & Microbe* **16** 276 – 289
- [103] Human Microbiome Project URL <https://hmpdacc.org/>
- [104] Qin J, Li R, Raes J, Arumugam M, Burgdorf K S, Manichanh C, Nielsen T, Pons N, Levenez F, Yamada T, Mende D R, Li J, Xu J, Li S, Li D, Cao J, Wang B, Liang H, Zheng H, Xie Y, Tap J, Lepage P, Bertalan M, Batto J M, Hansen T, Paslier D L, Linneberg A, Nielsen H B, Pelletier E, Renault P, Sicheritz-Ponten T, Turner K, Zhu H, Yu C, Li S, Jian M, Zhou Y, Li Y, Zhang X, Li S, Qin N, Yang H, Wang J, Brunak S, Doré J, Guarner F, Kristiansen K, Pedersen O, Parkhill J, Weissenbach J, Consortium M, Bork P, Ehrlich S D and Wang J 2010 *Nature* **464** 59–65
- [105] Ehrlich S D and the MetaHIT Consortium 2011 MetaHIT: The European Union Project on Metagenomics of the Human Intestinal Tract *Metagenomics of the human body* (K. Nelson ed.) (Springer Science+Business Media) chap 15
- [106] MetaHIT Website URL <http://www.metahit.eu>
- [107] Li J, Jia H, Cai X, Zhong H, Feng Q, Sunagawa S, Arumugam M, Kultima J R, Prifti E, Nielsen T, Juncker A S, Manichanh C, Chen B, Zhang W, Levenez F, Wang J, Xu X, Xiao L, Liang S, Zhang D, Zhang Z, Chen W, Zhao H, Al-Aama J Y, Edris S, Yang H, Wang J, Hansen T, Nielsen H B, Brunak S, Kristiansen K, Guarner F, Pedersen O, Doré J, Ehrlich S D, Consortium M, Bork P and Wang J 2014 *Nature Biotechnology* **32** 834–841
- [108] Vetrovský T and Baldrian P 2013 *PLoS ONE* **8** e57923
- [109] Metabolomic Workbench URL <https://www.metabolomicsworkbench.org/>
- [110] Ribosome Database Project URL <http://rdp.cme.msu.edu/>
- [111] EZBioCloud URL <https://www.ezbiocloud.net/>
- [112] Shreiner A B, Kao J Y and Young V B 2015 *Current Opinion in Gastroenterology* **31** 69–75
- [113] Thursby E and Juge N 2017 *Biochemical Journal* **474** 1823–1836
- [114] Kim S, Kim N, Presson A P, Metzger M E, Bonifacino A C, Sehl M, Chow S A, Crooks G M, Dunbar C E, An D S, Donahue R E and Chen I S 2014 *Cell Stem Cell* **14** 473–485
- [115] Wu C, Li B, Lu R, Koelle S J, Yang Y, Jares A, Krouse A E, Metzger M, Liang F, Loré K, Wu C O, Donahue R E, Chen I S Y, Weissman I and Dunbar C E 2014 *Cell Stem Cell* **14** 486–499
- [116] Belderbos M E, Koster T, Ausema B, Jacobs S, Sowdagar S, Zwart E, de Bont E, de Haan G and Bystriykh L V 2017 *Blood* **129** 3210–3220
- [117] Hebert P D, Cywinska A, Ball S L and deWaard J R 2003 *Proceedings of the Royal Society of London. Series B: Biological Sciences* **270** 313–321
- [118] Hebert P D N, Stoeckle M Y, Zemplak T S and Francis C M 2004 *PLoS Biology* **2** e312
- [119] Ratnasingham S and Hebert P D N 2007 *Molecular Ecology Notes* **7** 355–364
- [120] The Barcode of Life Data System URL <http://www.barcodinglife.org>
- [121] Kress W J, Wurdack K J, Zimmer E A, Weigt L A and Janzen D H 2005 *Proceedings of the National Academy of Sciences* **102** 8369–8374
- [122] Sgamma T, Masiero E, Mali P, Mahat M and Slater A 2018 *Frontiers in Plant Science* **9** 1828
- [123] Bruno A, Sandionigi A, Agostinetto G, Bernabovi L, Frigerio J, Casiraghi M and Labra M 2019 *Genes* **10** 248
- [124] Hawkins J A, Jones S K, Finkelstein I J and Press W H 2018 *Proceedings of the National Academy of Sciences* **115** E6217–E6226
- [125] Thielecke L, Aranyosy T, Dahl A, Tiwari R, Roeder I, Geiger H, Fehse B, Glauche I and Cornils K 2017 *Scientific Reports* **7** 43249
- [126] Tambe A and Pachter L 2019 *BMC Bioinformatics* **20** 32
- [127] Sun J, Ramos A, Chapman B, Johnnidis J B, Le L, Ho Y J, Klein A, Hofmann O and Camargo F D 2014 *Nature* **514** 322–327
- [128] Wu C, Li B, Lu R, Koelle S, Yang Y, Jares A, Krouse A, Metzger M, Liang F, Lore K and Wu C 2014 *Cell Stem Cell* **14** 486–499
- [129] Perié L and Duffy K R 2016 *FEBS letters* **590** 4068–4083
- [130] Blundell J R and Levy S F 2014 *Genomics* **104** 417 – 430
- [131] Rogers Z N, McFarland C D, Winters I P, Seoane J A, Brady J J, Yoon S, Curtis C, Petrov D A and Winslow M M 2018 *Nature Genetics* **50** 483–486
- [132] Akimov Y, Bulanova D, Abyzova M, Wennerberg K and

- Aittokallio T 2019 *bioRxiv*
- [133] Koelle S J, Espinoza D A, Wu C, Xu J, Lu R, Li B, Donahue R E and Dunbar C E 2017 *Blood* **129** 1448–1457
- [134] Xu S, Kim S, Chen I S and Chou T 2018 *PLoS computational biology* **14** e1006489
- [135] Dessalles R, D’Orsogna M and Chou T 2018 *Journal of Statistical Physics* **173** 182–221
- [136] Xu S 2018 *Mathematical Modeling of Clonal Dynamics in Primate Hematopoiesis* Ph.D. thesis UCLA
- [137] Biasco L, Pellin D, Scala S, Dionisio F, Basso-Ricci L, Leonardelli L, Scaramuzza S, Baricordi C, Ferrua F, Cicalese M P *et al.* 2016 *Cell Stem Cell*
- [138] Lythe G, Callard R E, Hoare R L and Molina-París C 2016 *Journal of Theoretical Biology* **389** 214–224 ISSN 0022-5193
- [139] Zarnitsyna V, Evavold B, Schoettle L, Blattman J and Antia R 2013 *Frontiers in Immunology* **4** ISSN 1664-3224
- [140] Yates A J 2014 *Frontiers in Immunology* **5** 13
- [141] Casrouge A, Beaudoin E, Dalle S, Pannetier C, Kanellopoulos J and Kourilsky P 2000 *Journal of Immunology* **164** 5782–5787
- [142] Keane C, Gould C, Jones K, Hamm D, Talaulikar D, Ellis J, Vari F, Birch S, Han E, Wood P, Le-Cao K A, Green M R, Crooks P, Jain S, Tobin J, Steptoe R J and Gandhi M K 2017 *Clinical Cancer Research* **23** 1820–1828
- [143] Sethna Z, Elhanati Y, Dudgeon C R, Callan C G, Levine A J, Mora T and Walczak A M 2017 *Proceedings of the National Academy of Sciences* **114** 2253–2258
- [144] Oakes T, Heather J M, Best K, Byng-Maddick R, Husovsky C, Ismail M, Joshi K, Maxwell G, Noursadeghi M, Riddell N, Ruehl T, Turner C T, Uddin I and Chain B 2017 *Frontiers in Immunology* **8**
- [145] Aguilera-Sandoval C R, OYang O, Jovic N, Lovato P, Chen D Y, Boechat M I, Cooper P, Zuo J, Ramirez C, Belzer M, Church J A, and Krogstad P 2017 *AIDS* **30** 701–711
- [146] Lythe G and Molina-París C 2018 *Immunological Reviews* **285** 206–217
- [147] Xu S and Chou T 2018 *Journal of Physics A: Mathematical and Theoretical* **51** 425602
- [148] Marcou Q, Mora T and Walczak A M 2018 *Nature Communications* **9** 561
- [149] Sethna Z, Elhanati Y, Callan Curtis G J, Walczak A M and Mora T 2019 *Bioinformatics* ISSN 1367-4803
- [150] Dessalles R, D’Orsogna M and Chou T 2019 *submitted to: PLoS Computational Biology*
- [151] Johnson P, Yates A, Goronzy J and Antia R 2012 *Proceedings of The National Academy of Sciences USA* **109** 21432–21437
- [152] Rane S, Hogan T, Seddon B and Yates A J 2018 *PLoS Computational Biology* **16** e2003949
- [153] Lewkiewicz S, Chuang Y L and Chou T 2018 *Bulletin of Mathematical Biology*
- [154] Egorov E S, Kasatskaya S A, Zubov V N, Izraelson M, Nakonechnaya T O, Staroverov D B, Angius A, Cucca F, Mamedov I Z, Rosati E, Franke A, Shugay M, Pogorelyy M V, Chudakov D M and Britanova O V 2018 *Frontiers in Immunology* **9** 1618
- [155] den Braber I, Mugwagwa T, Vrisekoop N, Westera L, Mögling R, Bregje de Boer A, Willems N, Schrijver E H R, Spierenburg G, Gaiser K, Mul E, Otto S A, Ruiter A F C, Ackermans M T, Miedema F, Borghans J A M, de Boer R J and Tesselaar K 2012 *Immunity* **36** 288–297
- [156] Maignan C, Ottaviano G, Pinelli D and Rullani F 2003 *Fondazione Eni Enrico Mattei*
- [157] Gini C 1912 *Reprinted in Memorie di metodologica statistica (Ed. Pizetti E, Salvemini, T). Rome: Libreria Eredi Virgilio Veschi*
- [158] Gastwirth J L 1972 *The Review of Economics and Statistics* **54** 306–316
- [159] Atkinson A B and Micklewright J 1992 *Economic transformation in Eastern Europe and the distribution of income* (Cambridge University Press)
- [160] Kennedy B P, Kawachi I and Prothrow-Stith D 1996 *Bmj* **312** 1004–1007
- [161] Theil H 1972 *Statistical decomposition analysis; with applications in the social and administrative sciences* Tech. rep.
- [162] Novotný J 2007 *The Annals of Regional Science* **41** 563–580
- [163] Lasarte E, Paniagua M A M *et al.* 2014 *Decomposition of regional income inequality and neighborhood component: A spatial Theil Index* Tech. rep. Instituto Valenciano de Investigaciones Económicas, SA (Ivive)
- [164] D’Ambrosio C and Wolff E N 2006 *Is Wealth Becoming More Polarized in the United States? International Perspectives on Household Wealth* Chapters (Edward Elgar Publishing) chap 12
- [165] Dambrosio C 2001 *Review of Income and Wealth* **47** 43–64
- [166] Wang Y Q and Tsui K Y 2000 *Journal of Public Economic Theory* **2** 349–363
- [167] Wolfson M C 1994 *American Economic Review* **84** 353–358
- [168] Bailey K D 1990 *Systems practice* **3** 365–382
- [169] Lewis J E, DeGusta D, Meyer M R, Monge J M, Mann A E and Holloway R L 2011 *PLOS Biology* **9** 1–6